Experimental evidence of twin-planes pinning in the *ab* plane studied in large *c*-axis $YBa_2Cu_3O_7$ samples

S. Sanfilippo
Elaboration par Procédés Magnétiques-Matformag, Centre National de la Recherche Scientifique, 25 Avenue des Martyrs, 38042 Grenoble Cedex 9, France

A. Sulpice and O. Laborde
Centre de Recherches sur les Très Basses Températures, Centre National de la Recherche Scientifique, 25 Avenue des Martyrs, 38042 Grenoble Cedex 9, France

D. Bourgault
Elaboration par Procédés Magnétiques-Matformag, Centre National de la Recherche Scientifique, 25 Avenue des Martyrs, 38042 Grenoble Cedex 9, France

Th. Fournier
Centre de Recherches sur les Très Basses Températures, Centre National de la Recherche Scientifique, 25 Avenue des Martyrs, 38042 Grenoble Cedex 9, France

R. Tournier
Elaboration par Procédés Magnétiques-Matformag, Centre National de la Recherche Scientifique, 25 Avenue des Martyrs, 38042 Grenoble Cedex 9, France

(Received 9 March 1998)

The twin-planes (TP) effect on pinning is studied in large monodomain $YBa_2Cu_3O_7$ textured samples with the size along the *c* axis greater than the others. The magnetic field angular dependence of the *c*-axis resistivity and *c*-axis critical current density has been carried out using transport and dc-magnetization measurements. These various experimental methods show clearly that in this configuration TP's dominate the pinning properties in the *ab* planes at high temperatures ($T \geqslant 40$ K) and when the magnetic field is close to the TP directions. Moreover, experiments demonstrate that the TP's enhance the *ab*-plane irreversibility line for angles close to a critical angle $\Phi_c \sim 8° - 10°$. The observed properties are related to the extended and correlated character of the twin planes. An experimental phase diagram for the angular dependence of the *ab*-plane irreversibility line is proposed with a possible existence of a Bose glass phase in the *ab* plane induced by the two directions of the TP's. The persistence of the TP pinning for magnetic fields higher than 20 T is explained with an electromagnetic origin induced by the surface character of TP's. [S0163-1829(98)08241-1]

I. INTRODUCTION

The understanding of the pinning of the flux lines in high-T_c superconductors has a fundamental as well a strong technological interest. From the fundamental point of view, it has been demonstrated that the magnetic phase diagram contains a rich and complex variety of new phases whose properties depend on the nature of the defects in the material.[1] Due to high thermal fluctuations and the short coherence length, a large part of the phase diagram is occupied by vortices in the liquid state.[2] Lowering the temperature, the liquid transforms in a vortex lattice in the case of pure single crystals or freezes in a glass whose character depends on the number and the type of the pinning sites.[3] For random distributed defects, a vortex glass phase is expected,[4] and in the case of extended correlated disorder, the low-temperature phase is predicted to be a Bose glass phase.[5] From the practical point of view, many applications require high current densities with minimal energy dissipation. Thus a strategy to improve the superconducting properties is to find the type of pinning site which immobilizes the flux line in the best way. Pinning by extended defects is very efficient because a considerable portion of the length of the vortices is localized on these pins. It has been observed that dislocations[6] or columnar defects created by heavy ion irradiation[7] or fission[8] are good candidates: they enhance the critical current and the irreversibility line due to their extended and correlated characters.[9]

The twin planes (TP's) in $YBa_2Cu_3O_7$ (YBCO) are a significant source of correlated disorder too.[10] They are inherent in the 123 materials, and their pinning effects can be studied without altering the superconducting properties of the material, as in the case of irradiated samples.[11] The role of TP's in flux line pinning has been the subject of an intense research on single crystals, textured materials, and thin films. Various techniques like resistivity,[12] magnetization,[13] and transport critical current density[14] measurements, scanning transmission electron microscopy (STEM),[15] and magneto-optic visualization techniques[16] already demonstrated clearly that TP's play a key role in transversal flux motion and flux pin-

ning for magnetic fields directed along the *c* axis. The mechanism usually proposed for pinning is still an open question. Twin boundaries are oxygen-deficient regions (i.e., locally antiferromagnetically insulating regions) with a width of the order of the coherence length. An attraction of the flux lines by the TP's due to a local depression of the order parameter is expected and pinning by a core effect is possible.[17] Another origin of pinning may stem from the extended and correlated nature of TP's.[3] Pinning by correlated disorder is stronger because it is less sensitive to thermal fluctuations. Thus the maximum contribution of TP's on pinning is expected to occur at high temperatures, in fact above the so-called depinning temperature T_{DP}.[3] However, in samples when strong point disorder and extended defects are present, the situation is more complex. Theoretically, scaling arguments suggest that a Bose glass phase cannot be stable,[18] while experimentally Safar *et al.*[19] show that in YBCO thick films the vortices freeze in a Bose glass due to the correlated properties of the TP's in the *c*-axis direction.

In this paper the effectiveness of TP's on pinning versus point disorder is studied in an original configuration. We investigate the pinning by TP's for vortices in the *ab* plane in high quality bulk textured bars. The samples are single-domain twinned in the two directions, with the existence of many twin intersection areas. Unlike the case of single crystals, the experiments are carried out in samples with the *c*-axis size greater than the other ones. The important *c*-axis length (3 mm) allows one to perform direct *c*-axis transport critical current and resistive measurements. Transport and magnetic measurements are carried out with *B* always lying in the *ab* plane. This suitable geometry permits one to get rid of the influence of the anisotropy between the *ab* plane and the *c* axis which could mask TP effects in the measurements. A strong influence of the twin planes on the *c*-axis critical current density, the *c*-axis resistivity, and the *ab*-plane irreversibility line is reported for a field intensity up to 20 T, close to the TP directions.

II. EXPERIMENTAL DETAILS

Textured bulk samples of Y-Ba-Cu-O have been prepared using the top-seed melt-texturing method.[20] The starting composition was Y-123 with the addition of 30 wt. % of Y_2BaCuO_5, and the seeds used were single crystals of $SmBa_2Cu_3O_7$. The microstructure of the monodomain textured samples shows the presence of well-dispersed spherical or needlelike grains of Y_2BaCuO_5 (Y-211) with a typical size and interspacing of a few micrometers throughout the entire volume. The density of these Y-211 particles is estimated to be around 30% of the volume by measuring the paramagnetic susceptibility of the sample and of the Y-211 pure phase. Bars with typical dimensions of 3 mm length and 0.4 mm^2 cross section are cut with the crystallographic axis parallel to the sides of the sample. X-ray pole figures obtained using the Schulz reflection method,[21] confirm the high quality of the texture and the crystallographic orientations of the samples. The mosaicity of the *c*-axis orientation obtained by (006) rocking curves using inelastic neutron scattering is around 1.5°.[22] The samples are then annealed at 420 °C in flowing oxygen during 72 h. Our samples are twinned with a high density of twinned domains, domains which are regions

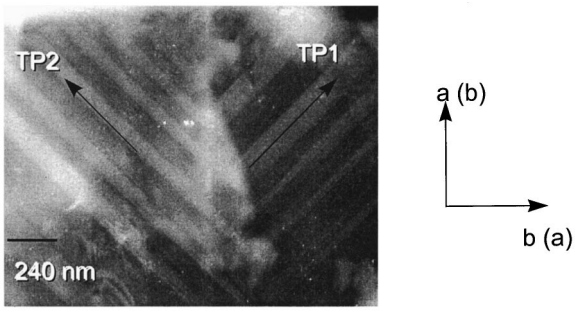

FIG. 1. TEM micrograph performed along [001] showing an intersection between the two TP directions (TP1, TP2) in the *ab* plane.

where the twin boundaries all have the same orientation. This can be due to the presence of a high density of Y-211 particles since it has been proposed that Y-211 particles could be nucleation centers for twinning domains.[23] The widths of the twin domains are variable, and the mean value ranges from 5 to 20 μm in the *ab* plane as has been observed on optical micrographs. Twin domain coherence is small since it is limited by the 211 particles or by the overlapping of two sets of twins. The intersections between the two families can even form a canvas[24] as we can see in Fig. 1 where TP1 and TP2 are the name of the two twin-plane families. This type of intersection always represents a pinning center and reduces the channeling phenomena (or guides the vortices by the TP's) observed in single crystals with one twin-plane family.[25] An average distance of 1000 Å between the twin planes has been estimated by TEM, although some local variations exist due to variations of the Y-211 density and associated strain fields (Fig. 1). The structural width of these planar defects has not been determined in our samples, but it usually lies between 10 and 50 Å.[26,27] For calculation we choose an intermediate value of the thickness: $2*t_{TP} = 30$ Å, where t_{TP} is the half thickness.

Transport measurements (critical current and resistive measurements) are performed using the standard four-probe configuration. The contacts are made with silver paint and briefly annealed at 900 °C. Transport critical currents are measured at 77 K with an electric field criterion of 10 μV/cm.

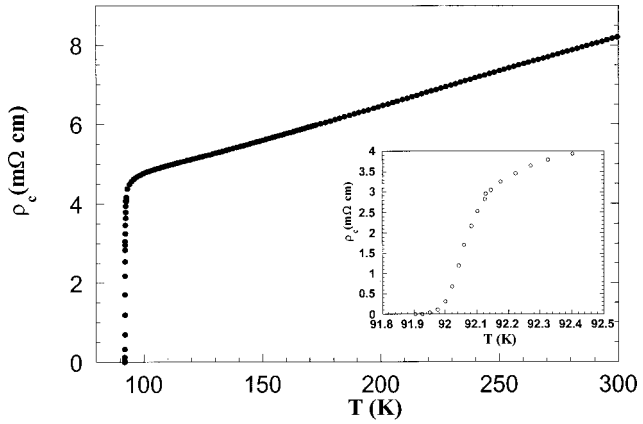

FIG. 2. *c*-axis resistivity as function of the temperature in zero applied field. Inset: superconducting transition for a typical sample in zero applied field ($T_c = 91.9$ K).

We made *c*-axis resistive measurements in the same samples with the same configuration using the standard four-probe technique with low-frequency (33 Hz) ac currents. The current density is about 0.13 A/cm^2. The characterization has been carried out in a magnetic field intensity up to 20 T at the Grenoble High Magnetic Fields Laboratory. Figure 2 shows the resistivity as a function of the temperature in zero magnetic field. A $T_c = 91.9$ K and a transition width $\Delta T_c < 200$ mK are observed. The shape of $\rho_c(T)$ in the normal state is linear down to T_c, and the values of the resistivity at 300 and 100 K which are $\rho_c(300\,\mathrm{K}) \sim 8.2\ \mathrm{m\Omega\,cm}$ and $\rho_c(100\,\mathrm{K}) \sim 4.8\ \mathrm{m\Omega\,cm}$, respectively, are similar to what is observed for well-oxygenated single crystals.[28]

We performed dc magnetization measurements $M(B)$ and $M(T)$ curves for T between 40 and 90 K and with a field intensity up to 7 T in a commercial superconducting quantum interference device (SQUID) magnetometer, allowing the rotation of the sample around the *c* axis in steps of 2°. We have used the $M(B)$ hysteresis cycles to extract the *c*-axis critical current density $J_c^{\mathrm{magn}(c\ \mathrm{axis})}$. Here $J_c^{\mathrm{magn}(c\ \mathrm{axis})}$ has been calculated from the differences of magnetization between the upper and lower branches of the hysteresis loops (ΔM) and with the help of the extended Bean model developed by Gyorgy *et al.*[29] to take into account the anisotropy between the *c* axis and *ab* planes. Following this model, the critical current densities along the *c* axis, $J_c^{\mathrm{magn}(c\ \mathrm{axis})}$, and in the *ab* plane, $J_c^{\mathrm{magn}(ab\ \mathrm{plane})}$, are related to ΔM by

$$\Delta M = \frac{J_c^{\mathrm{magn}(c\ \mathrm{axis})} \cdot l_{ab}}{20}\left[1 - \frac{l_{ab}}{3l_c}\frac{J_c^{\mathrm{magn}(c\ \mathrm{axis})}}{J_c^{\mathrm{magn}(ab\ \mathrm{plane})}}\right],$$

where l_{ab} and l_c are, respectively, the size of the sample along the *ab* plane and along the *c* axis. Note that in this geometrical configuration $l_c > l_{ab}$ and that $J_c^{\mathrm{magn}(ab\ \mathrm{plane})} \gg J_c^{\mathrm{magn}(c\ \mathrm{axis})}$,[30] yielding $\Delta M = (J_c^{\mathrm{magn}(c\ \mathrm{axis})} \cdot l_{ab})/20$. So in that case the critical current studied is limited by the *c* axis one. Using $M(B)$ cycles obtained at different temperatures, we also study the variation of $\Delta M(T)$ for various angles between the field and TP directions in the *ab* plane.

The irreversibility points $T_{\mathrm{irr}}(B)$ were obtained from splitting the $M(T)$ curves measured under zero-field-cooled and field-cooled conditions. The determination of T_{irr} is carried out in the same experimental conditions for each angle and each field intensity up to 7 T.

III. RESULTS AND DISCUSSION

A. *c*-axis transport critical current

The experimental configuration is presented Fig. 3. The dc current is directed along the *c* axis, and the magnetic field is applied in the *ab* planes, making a variable angle Φ with one TP direction. The angular dependence was explored by rotating the sample around the *c* axis with a rotation step of 2°. The measurements were performed at 77 K for fields ranging from 0 to 8 T using the constant Lorentz force configuration $B \perp I$. Figure 4 shows the behavior of $J_c^{\mathrm{tr}}(\Phi)$ for different magnetic fields $B \geqslant 1$ T and when it is rotated in the *ab* plane. $J_c^{\mathrm{tr}}(\Phi)$ curves exhibit two identical sharp peaks at $\Phi = 0$ and 90° (corresponding to the TP directions), having an angular width of about $\Phi_c \sim 10°$. The peaks correspond to the same critical current density of 6500 A/cm^2, although due to the complex microstructure of the samples where several types of pinning coexist (point defects, linear defects like dislocations, planar defects like stacking faults) (Ref. 31) these peaks indicate clearly that at 77 K in this configuration ($B \| ab$ plane, $I \| c$ axis) the twin planes are the dominant source of pinning in the sample. Indeed, for fields $\geqslant 6$ T, the $J_c^{\mathrm{tr}}(\Phi = 0°)$ for B parallel to the twin planes is 6 times greater than $J_c^{\mathrm{tr}}(\Phi > \Phi_c)$. In addition, a small enhancement of $J_c^{\mathrm{tr}}(\Phi)$ is observed for $\Phi = 45°$, corresponding to the pinning by the crossing points of the twin boundaries in the *ab* plane.

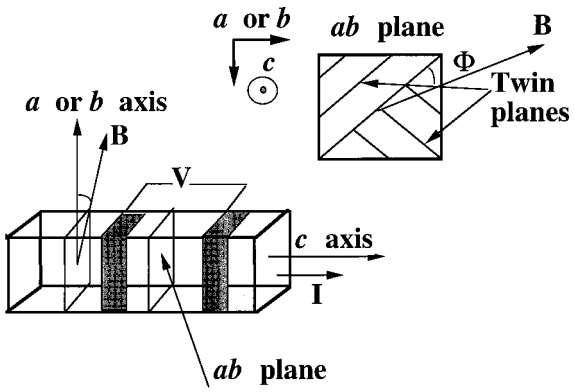

FIG. 3. Configuration used for transport measurements: the current is directed in the *c* axis and B is applied in the *ab* plane. Φ is the variable angle between B and one TP direction.

This angular shape of $J_c^{\mathrm{tr}}(\Phi)$ indicates the existence of a critical angle Φ_c corresponding to the onset of the flux lines trapped by the twin planes. This critical angle is determined by the balance between the vortex line tension for free (ε_0) and trapped segments in the TP's ($\varepsilon_{\mathrm{TP}}$): $\cos\Phi_c \sim (\varepsilon_{\mathrm{TP}}/\varepsilon_0)$.[32] For $0 < \Phi \leqslant \Phi_c$ a partial accommodation of the flux lines by the TP's occurs, producing a kinked structure between planes of the same twin family with one part of the segments locked to the TP's. Here $J_c^{\mathrm{tr}}(\Phi)$ decreases slowly in this angular range due to the motion of vortices along the TP's induced by the field component perpendicular to the twin plane direction. For $\Phi > \Phi_c$ twin planes pinning disappears and flux lines follow the direction of B. Here J_c^{tr}

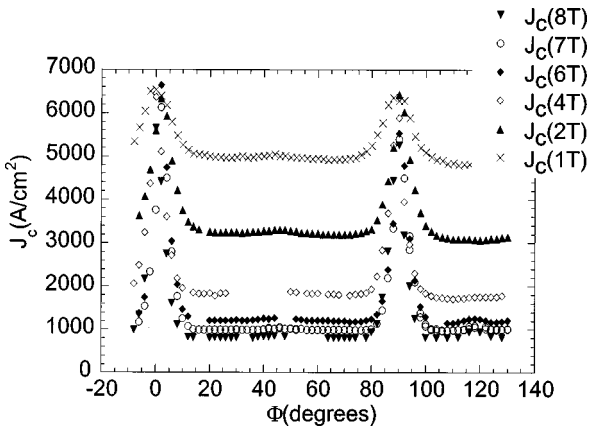

FIG. 4. Angular dependence of the *c*-axis transport J_c for B applied in the *ab* plane between 1 and 8 T.

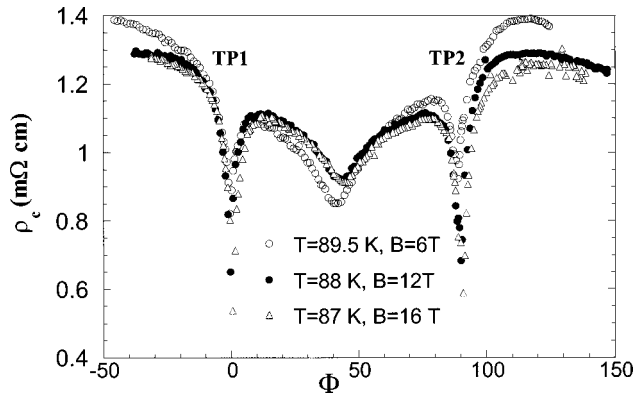

FIG. 5. Angular variation of the *c*-axis resistivity for *B* applied in the *ab* plane for field intensity up to 16 T.

($\Phi > \Phi_c$) is determined by the pinning of the defects of the bulk. A complete study of the physical phenomena for fields between 0 and 8 T is published elsewhere.[33]

B. *c*-axis resistivity

The *c*-axis resistivity measurements have been realized using the same configuration as for J_c transport measurements. With a current applied in the *c*-axis direction, a rotation of the magnetic field in the *ab* plane has been also realized. The angle $\Phi = 8°$ is still defined when *B* is aligned with one twin-plane direction. The samples used are cut with the edges of the face containing the *ab* plane, making an angle of 30° with one TP family. We performed first resistive angular measurements at constant temperature and fields. Then we studied the variation of the resistivity versus field for several temperatures and two angles, $\Phi = 0$ and $\Phi = 8°$. Figure 5 shows the behavior of the normalized *c*-axis resistivity $\rho_c(\Phi)$ as a function of the angle of the magnetic field with respect to one twin-plane direction for three temperatures and fields ($T = 89.5$ K, $B = 6$ T; $T = 88$ K, $B = 12$ T; $T = 87$ K, $B = 16$ T). Remarkably, the $\rho_c(\Phi)$ curves are the inverted images of the *c*-axis $J_c^{\mathrm{tr}}(\Phi)$ curves. We observed two sharp drops of the magnetoresistivity when *B* is directed parallel to the TP's up to fields larger than 16 T. The reduction of the resistivity by TP pinning is huge (7.5∼ mΩ cm for $B = 16$ T and $T = 87$ K), but disappears for a critical angle Φ_c around 88°. This depinning angle does not shrink even at a high field intensity of 20 T. Moreover, a third dip in resistivity appears for $\Phi = 45°$, that is, when *B* is directed at the intersection of the two-twin-boundary family. Note that such a minimum does not exist for $\Phi = 135°$.

The curves $\rho_c(B)$ measured for $\Phi = 0$ and $\Phi = \Phi_c$ and for three temperatures [Figs. 6(a), 6(b), and 6(c)] confirm clearly the strong reduction of dissipation induced by TP pinning. The onset of pinning occurs in the lower part of the transition, below 2 mΩ cm, which is approximately 44% of ρ_c (100 K). However, this is well in the region where the vortex state is expected to be a liquid.[34] The resistivity reduction does not disappear with increasing the intensity of the magnetic field, but becomes stronger. The maximum of $\Delta\rho_c$ is characterized by a shoulder in the ρ_c $(B, \Phi = \Phi_c)$ curves, which does not exist for $\Phi = 0°$. Moreover, at $T = 86.5$ K, the TP pinning is so strong that it pushes the experimental zero resistivity to a higher magnetic field of 0.8 T [inset of

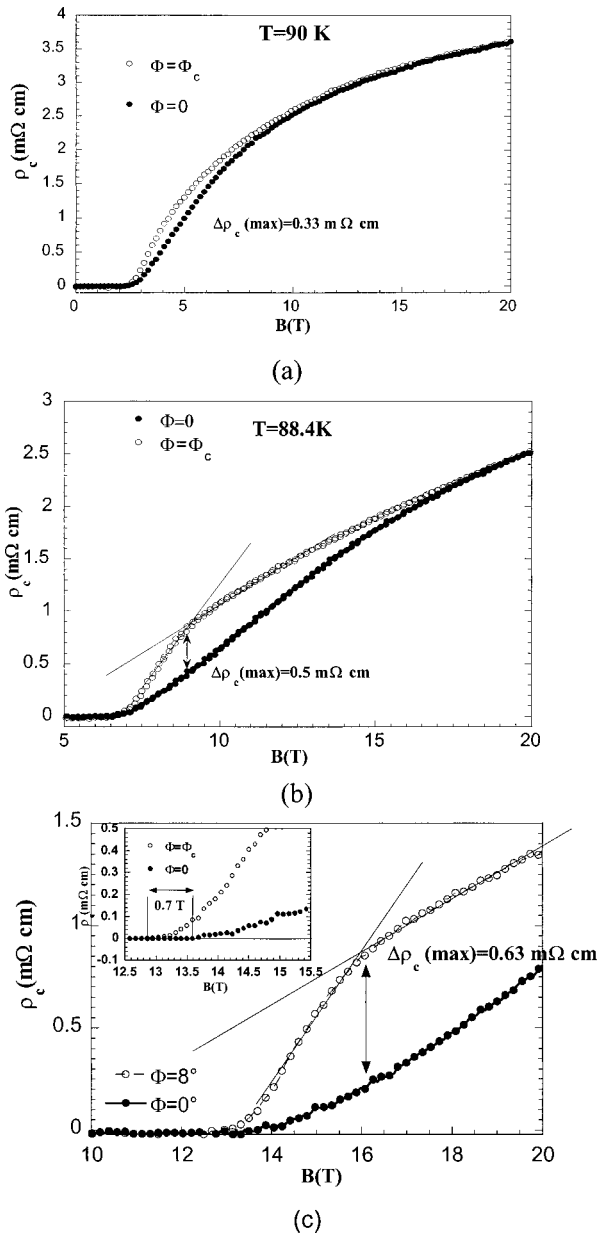

FIG. 6. Magnetoresistivity vs fields intensity up to 20 T for $\Phi = 0$ and Φ_c. (a) for $T = 90$ K, (b) for $T = 88.4$ K, and (c) for $T = 86.45$ K. Note that the three parts of the figure are not in the same scale. Inset to (c): comparison between the experimental zero resistivity for $\Phi = 0$ and Φ_c.

Fig. 6(c)]. Note that the resistivity is Ohmic in the range where it can be measured, suggesting that the transition toward the glass state lies below our experimental zero.

We observe here some similar features reported in the case of single crystals for twin planes or columnar irradiation when *I* is directed in the *ab* plane and *B* parallel to the *c* axis.[35–37] The TP's localize the flux lines in the liquid state in the *ab* plane where the absence of the shear modulus limits the effectiveness of pinning. The persistence of this huge reduction of dissipation at very intense magnetic field is not clear, but we can consider two hypotheses. First, we have to remember the existence of two directions of twinning and areas of intersections between the two families. In a certain sense we can make an analogy with the case of crossed or splayed irradiated columnar defects. It has been

theoretically[38] and experimentally[39] demonstrated that the crossing or the spreading in direction of the columnar defects forces a topological entanglement of the liquid state, strongly reducing vortex motion. The flux lines can be localized directly by a columnar defect, but also by the arrangement between adjacent tilted vortices (the exchange of many flux lines between two pins). Second, at high magnetic fields a large viscosity can arise from flux line entanglement. This large viscosity provides the effect of strong pinning centers like TP's to propagate over large distances in the flux liquid.[40] The existence of a third minima of ρ_c at 45° and not at 135° can have two origins. First, it could be due to the mosaicity of the orientation of the samples: the field would be really in the *ab* plane only in this direction. Another origin of the pinning in this direction can be the canvas formed by the intersections of the two TP families. The pinning arising by this kind of intersection is strong because the centers are in the case points which are correlated. Several optical micrographs indicate that this type of intersection occurs mostly in one direction (for $\Phi=45°$) and less in the other ($\Phi=135°$). This could explain the absence of a dip for $\Phi=135°$. To end with a resistive characterization we have to note here a difference with that observed in single crystals: the shoulder in the resistive curves does not appear when B is in the direction of the TP's but for $\Phi=\Phi_c$. Often, the kink at around 20% of ρ_n has been considered as a signature of twin-plane pinning.[34–36] In our experiments it has clearly another origin.

C. $J_c^{\mathrm{magn}(c\ \mathrm{axis})}(\Phi)$ at 77 K, $\Delta M(B)$, and $\Delta M(T)$

For magnetization measurements, the magnetic field is applied in the *ab* plane, still making the variable angle Φ with one twin-planes direction. ΔM versus B curves are performed for several angles at 77 K and for B between 1 and 7 T in order to compare with the direct *c*-axis transport J_c measurements. Then we proceed to the same experiments, but for T varying between 40 and 90 K to check the influence of the twin planes on thermal effects. In Fig. 7(a) we plot the width of the magnetization measurements for two orientations of the applied field B, namely, $\Phi=0$ (one direction of the twin plane) and $\Phi=45°$ at 77 K. We observe that the width of the magnetic hysteresis ΔM, which reflects the efficiency of the flux trapping, is significantly increased when B is along the twin planes for fields between 0.5 and 7 T. This enhancement occurs only when B is near a critical angle Φ_c around 8° with respect to the twin-plane directions [Fig. 7(b)]. When $B=7$ T, the extracted critical current density $J_c^{\mathrm{magn}(c\ \mathrm{axis})}$ is estimated for $\Phi=0$ ($B\|$TP) to be 10 times higher than for $\Phi=\Phi_c$. We found a good qualitative agreement with respect to the angular dependence observed for $J_c^{\mathrm{tr}}(\Phi)$. A quantitative difference in the critical current value by a factor of 2 between the two determinations is observed, attributed certainly to the difference of criteria between transport and magnetic measurements. At 77 K the field dependence of ΔM follows the law $\Delta M(B)=aB^{-\alpha}(1-B/B^*)$, where a is a constant [Figs. 8(a) and 8(b)]. To the usual power law field dependence in $B^{-\alpha}$, a linear term $(1-B/B^*)$ has also been introduced to take into account of the presence of the irreversibility line.[41] When B is directed to the twin planes, α is equal to 1/2. This is consistent with an interfacial pinning. Indeed, when the vortex interval a_0 is less than the twin spacing d_{TP}, the number N_p of the vortices pinned by the twin planes is inversely proportional to $a_0^* d_{\mathrm{TP}}$. The bulk pinning force per unit volume, F_p, is proportional to N_p and can be deduced by[42]

$$F_p=\frac{1}{a_0 d_{\mathrm{TP}}}\left(\frac{B_c^2}{\mu_0}\right)\xi, \quad \text{where} \left(a_0=\sqrt{\frac{\phi_0}{B}}\right),$$

and therefore has a $B^{1/2}$ dependence. As the critical current density can be calculated by $J_c=F_p/B$, J_c follows, in the case of planar defects, a $B^{-1/2}$ dependence. For $\Phi=45°$, α is closed to 1. This reflects pinning by all types of defects in the bulk.[43]

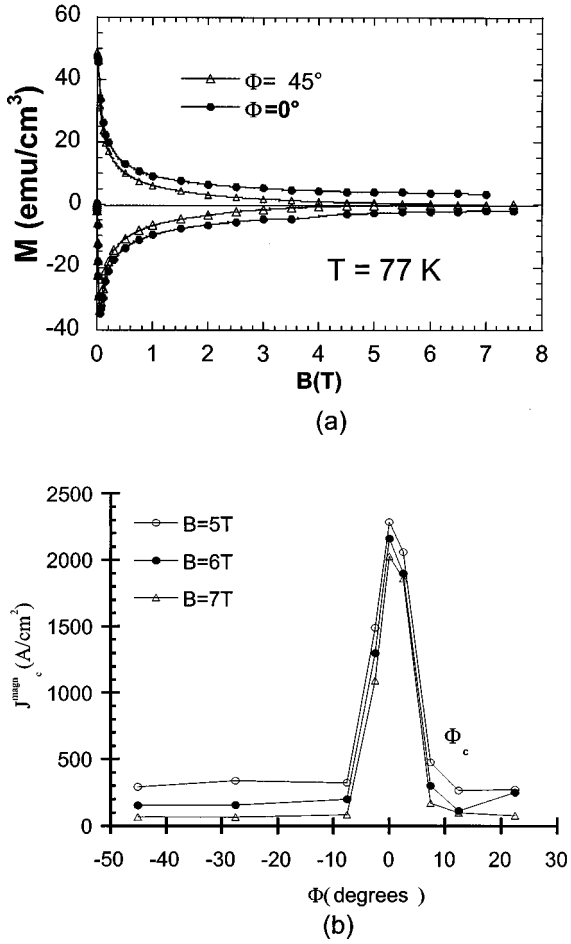

FIG. 7. (a) $M(B)$ hysteresis cycle for B between 0 and 7 T for $\Phi=0$ and 45°. (b) Angular dependence of $J_c^{\mathrm{magn}(c\ \mathrm{axis})}$ determined using the anisotropic Bean model.

Figures 9(a) and 9(b) show the hysteresis width ΔM at $B=1$ and 7 T as a function of the temperature at $\Phi=0$ and 45°. The comparison, Fig. 9(a), indicates that for B close to the TP direction the smoothing of ΔM (and hence of $J_c^{\mathrm{magn}(c\ \mathrm{axis})}$) by temperature effects is smaller than for $\Phi=458$. This can be qualitatively explained by the reduced dimensionality of thermal fluctuations for a flux line trapped in the TP's. Indeed, thermal fluctuations of the vortex position increase the range of the pinning force r_p ($r_p\sim\xi$ to $r_p\sim(\xi+\langle u^2\rangle_{\mathrm{th}})$ where $\langle u^2\rangle_{\mathrm{th}}$ represents the amplitude of the thermal displacement). This smoothes the effective pinning potential and reduces the collective pinning force. But J_c is

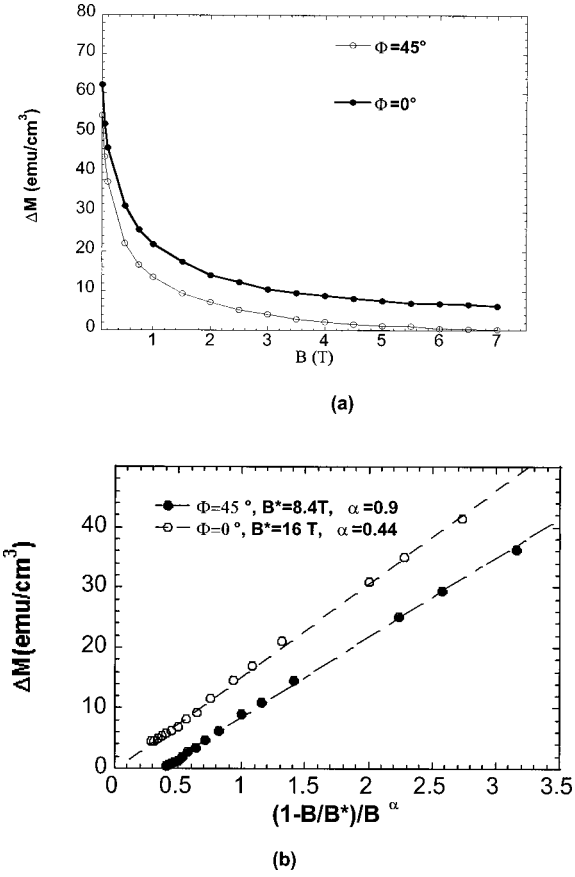

FIG. 8. (a) Field dependence of the hysteresis width ΔM at $T=77$ K for $\Phi=0$ and 45°. (b) $\Delta M(B)$ in a semilogarithmic representation fitted with $\Delta M(B)=AB^{-\alpha}(1-B/B^*)$.

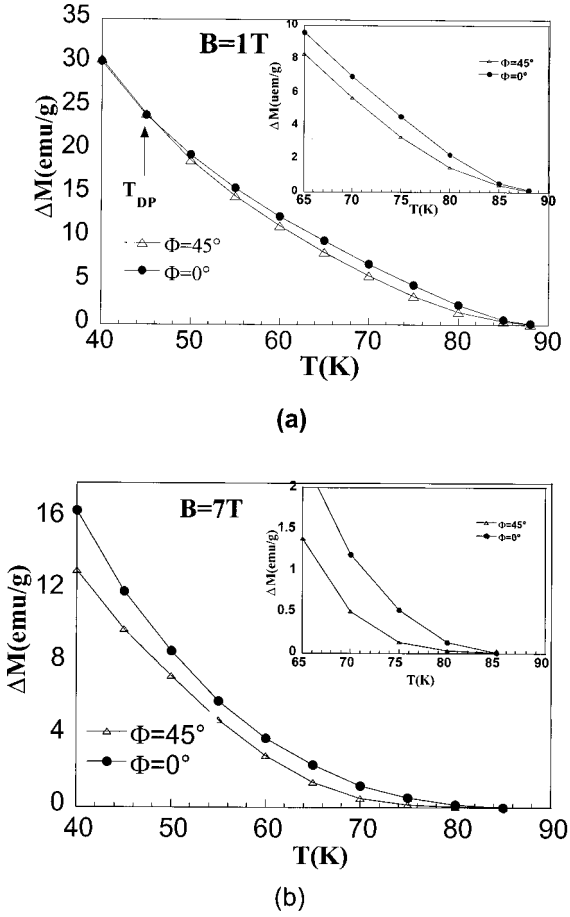

FIG. 9. (a), (b) Temperature dependence of the hysteresis width ΔM for $\Phi=0$ and 45° and fields $B=1$ and 7 T.

renormalized by thermal fluctuations differently depending on the nature of the pinning center. For point disorder the smoothing of J_c is exponentially strong with T (Ref. 44) because such disorder provides random walks of the flux lines to take advantage of locally favorable regions of impurities. On the contrary, planar defects suppress the transverse wandering (i.e., perpendicular to the TP's) of the vortices by attracting a large part of the flux lines to itself. Thus the critical current density for linelike defects (correlated defects) should be less affected by temperature.[10] For $B=1$ T the depinning temperature T_{DP} (above which the flux line begins to wander) is evaluated around 45 K, a little higher than the theoretical predictions (30 K).[45] For $B=7$ T the effect persists and T_{DP} is lower than 40 K.

D. Irreversibility line in the *ab* plane $I\cdot L_{ab}$

Figure 10 shows the irreversibility lines obtained for YBCO samples for fields applied perpendicularly to the c axis and directed along ($\Phi=0$) and 45°($\Phi=45°$) to the twin planes. Clearly, the point ($T=87$ K, $B=3$ T) divides two distinct behaviors. For $T=87$ K and low $B\leqslant 3$ T, the $I\cdot L_{ab}$ is isotropic, while for high fields ($B>3$ T) and low temperatures ($T<87$ K) the $I\cdot L_{ab}$ is anisotropic, following the same angular dependence observed for the c-axis critical current. When Φ is less than the critical angle Φ_c (=8°), $I\cdot L_{ab}$ moves clearly toward higher temperatures. An identical behavior is observed for the two twin-plane directions. When the field is parallel to TP's, the line is smooth and its position up to $B=7$ T is well described by the power law $B^*\propto(1-T/T_c)^{3/2}$. This suggests that the origin of pinning (i.e., the twin plane) is the same in all temperature and field ranges studied. On the other hand, when the angle between the field and TP direction is larger than Φ_c, $I\cdot L_{ab}$ presents a reproducible kink around $B=3$ T and $T=87$ K corresponding to a variation of slope, which suggests a change in the vortex matter or in the vortex pinning origin.

These experimental features can be understood as a consequence of the different responses at high temperatures to thermal fluctuations between correlated planar disorder and pointlike disorder. Still using the analogy of columnar defects, we try to explain the shape of $I\cdot L_{ab}$ and give an experimental phase diagram (Fig. 10). Let us begin with the origin of the anisotropy of $I\cdot L_{ab}$. For $T<87$ K and $B>3$ T, $I\cdot L_{ab}$ becomes anisotropic. It is shifted to lower field values when B is directed with an angle greater than Φ_c. This is similar to what is observed in the case of correlated defects induced by heavy ion irradiation along the c axis. Indeed, a ''cusp'' of the irreversibility line when B is close to the c axis has been observed[46,47] due to the existence of two distinct glass phases: a vortex glass phase and a Bose glass phase produced by competition between point and correlated disorder. These glasses have similar nonlinear dynamic characteristics, but differ by the response to a tilting of B.[48] On the one hand, the disorder associated with points defects is

isotropic. Close to the vortex glass phase transition, the correlated volume diverges isotropically and the irreversibility line in the *ab* plane should not be angle dependent. The disorder due to the TP's is anisotropic and correlated in direction point to point. Near the Bose glass phase transition, the correlation volume diverges with two different correlation lengths, leading to an anisotropy of the irreversibility line. In fact, the existence of a transition temperature into a Bose glass phase has been experimentally investigated only for extended defects along the *c* axis. To the best of our knowledge, there are no explicit predictions or any experimental investigations of a Bose glass caused by TP pinning in the *ab* plane. We propose that the pronounced difference in the angular dependence of $I \cdot L_{ab}$ when B is rotated through the critical angle Φ_c suggests the existence of two distinct glass phases in the *ab* plane too: a vortex glass phase for $\Phi > \Phi_c$ and a Bose glass phase for $\Phi \leqslant \Phi_c$ whose transition is tracked by the irreversibility lines named $B(T_{\mathrm{VG}})$ and $B(T_{\mathrm{BG}})$ in Fig. 10. For $\Phi > \Phi_c$ the region (labeled IV) is a vortex glass phase induced by point disorder (oxygen vacancies, impurities) and characterized by a random and enhanced wandering of flux lines. Due to their flexibility, the vortex lines wander significantly as they pass through the sample in high-T_c superconductors.[49] When $\Phi \leqslant \Phi_c$ correlated disorder (twin planes) suppresses the wandering, localizes the vortices, and forms a Bose glass phase with a wider irreversible region (region labeled III). In fact, in our case, the low-temperature phase may not be a true Bose glass phase. Because of the existence of many crossing points between the twin planes, it could have some properties observed in the glassy state induced by a splay of columnar defects. The benefits of the crossing of the defects is to reduce the dissipation due to the flux creep effect by precluding the expansion of double kinks.[50,51]

Another interesting feature is that we observe an increasing effect on $I \cdot L_{ab}$ at high fields when a huge fraction of vortices is not trapped at the TP's. Such an extension to high fields (9 T) has already been observed by Safar *et al.* in thick YBCO films.[19] It has been suggested that vortex-vortex interaction favors the blocking of the interstitials vortices by those pinned in the twin planes, producing a caging effect.[19] Another explanation is to remember the surface character of the TP's. In addition to the usual core pinning, the interaction between the TP's and the vortices should take into account the effect of the vortex image, which could hinder the flux line movement on the length scale of the magnetic penetration depth. The influence of such internal surfaces at high fields has been brought to the fore by *ab*-plane transport critical current density measurements.[14] More recently, a concentration of vortices near the TP's on two or three vortex spacings possibly induced by magnetic pinning has been observed by STEM visualization.[11]

We now discuss the part of the phase diagram separated by an isotropic irreversibility line (regions labeled I and II) ($T > 87$ K, $B < 3$ T). The continuity of $I \cdot L_{ab}$ in this direction suggests that in the isotropic part of the irreversibility line, the irreversible behavior is dominated only by twin-plane pinning (region labeled II in Fig. 10). This can be explained as follows. Near T_c, a softening of the vortex lattice has been observed due to the reduction of the shear modulus c_{66}.[52] It improves the accommodation of the flux lines to the

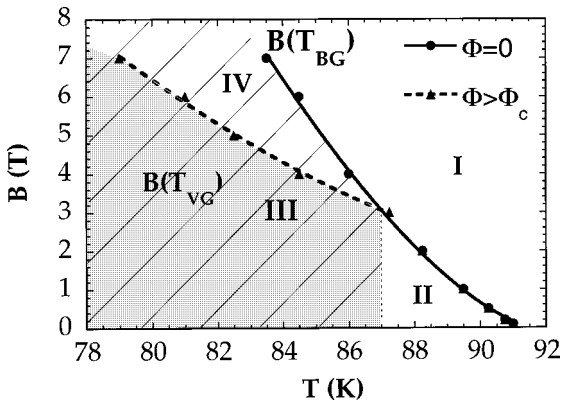

FIG. 10. Angular dependence of the *ab*-plane irreversibility line for B directed along and at 45° of one twin-plane direction. Note that for $\Phi > \Phi_c = 8°$ the irreversibility line is independent of the angle Φ. In the same figure, an experimental phase diagram B vs T for B applied in the *ab* plane and Φ between 0 and 45° is presented. Four regions are delimited. The dashed area represents the irreversible region for $\Phi < \Phi_c$ (region IV). The gray region represents the irreversible region where the pinning is dominated by point disorder (region III). Here $B(T_{\mathrm{BG}})$ and $B(T_{\mathrm{VG}})$ are the lines which determine the apparition of a Bose glass and a vortex glass phase, respectively.

defects and enhances the preferential pinning of the flux lines by planar defects like the twin planes. This occurs wherever the field is directed because flux lines depinned from the points defects will be trapped by the twin planes. The amplitude of thermal fluctuations $\langle u^2 \rangle_{\mathrm{th}}^{1/2}$ is so high that the pinning of flux lines is realized by many twin planes. If we apply for twin planes the approach of Nelson and Vinokur used for columnar defects,[53] the crossover to a collective pinning by many TP's is reached at a temperature T_{dl} where $\langle u^2 \rangle_{\mathrm{th}}^{1/2}$ is larger than the mean spacing between the twin planes. Following Nelson and Vinokur, this occurs when $T > T_{\mathrm{dl}}$, T_{dl} defined by the condition $\langle u^2 \rangle_{\mathrm{th}}^{1/2} = d_{\mathrm{TP}}$. Here T_{dl} can be calculated with the help of the formula

$$\frac{T_{\mathrm{dl}}}{T_c} \approx \frac{[t_{\mathrm{TP}}/4\xi_{ab}(0)][\sqrt{\ln(\kappa)/G_i}]\alpha}{1+[t_{\mathrm{TP}}/4\xi_{ab}(0)][\sqrt{\ln(\kappa)/G_i}]\alpha},$$

where G_i is the Ginzburg number (which is 0.01 in YBCO), κ is the Ginzburg-Landau parameter (that is 100 for YBCO), and t_{TP} the half of the average thickness of the twin plane ($\approx$15 Å). α is a number which depends on the intertwin distance and from the temperature T_1, where the wandering plays a significant role in determining the localization length:

$$\frac{T_1}{T_c} \approx \frac{(t_{\mathrm{TP}}/4\xi_{ab}(0))\sqrt{\ln(\kappa)/G_i}}{1+(t_{\mathrm{TP}}/4\xi_{ab}(0))\sqrt{\ln(\kappa)/G_i}} \approx 0.87$$

and

$$\alpha = \ln^{1/2}\left(\frac{d_{\mathrm{TP}}}{\sqrt{2}\xi_{ab}(0)}(1-T_1/T_c)^{1/2}\right).$$

With d_{TP} around 1000 Å, $T_c = 92$ K, we find a delocalization temperature T_{dl} of about 84 K. This is not so far from our experimental determination $T_{\mathrm{dl}} \sim 87$ K. So in the isotropic part of $I \cdot L_{ab}$, the flux lines are probably not pinned by an

individual planar defect, but by the collective action of many twin planes of the same family, when the local fluctuation of the density of TP's is favorable.

IV. CONCLUSIONS

In summary, we have shown that in bulk textured monodomain samples the twin planes are strong pinning centers which determine the superconducting properties measured in the *c*-axis direction when *B* is in the *ab* plane and close to the TP's. Pinning properties are increased at high temperatures ($T>40$ K) in a small angular range near the TP direction (8°–108°). The TP effect enhances the critical current density characterized by two peaks in the transport measurements and a larger magnetic hysteresis width. TP's also reduce the *c*-axis dissipation, inducing two dips in the *c*-axis resistivity curves, making the $\Delta M(T)$ curves less sensitive to thermal fluctuation and increasing the *ab*-plane irreversibility line. In these samples where point disorder is strong and competes with correlated disorder, the role played by the TP's is double: in the liquid state they localize the flux lines and reduce the dissipation for field up to 20 T. It also modifies the glassy state for $T<87$ K and $B>3$ T and may induce a Bose glass phase in the *ab* plane up to a field intensity of 7 T. The observed effects are attributed to a dimensional reduction of the thermal fluctuations for flux lines trapped in the planes. Moreover, the persistence of the phenomena when the vortices outnumber the TP's opens the question of the nature of the interaction between these internal surfaces and the flux lines. The results presented here show clearly that the control of the TP density in melt textured compounds is crucial for future applications of YBCO in the *c*-axis direction.

ACKNOWLEDGMENTS

The authors would like to thank X. Chaud and P. Gautier Picard for providing the YBCO monodomain samples. We would also like to thank P. Germi of the Laboratoire de Cristallographie of CNRS Grenoble for the pole figures. Discussions with C. Villard, X. Obradors, and H. C. Freyhardt are gratefully acknowledged.

[1] D. S. Fisher, M. P. A. Fisher, and D. Huse, Phys. Rev. B **43**, 130 (1991).
[2] D. R. Nelson and S. Seung, Phys. Rev. B **39**, 9153 (1989).
[3] For a topical review, see G. Blatter, M. V. Feigel'man, V. B. Geshkenbein, A. I. Larkin, and V. M. Vinokur, Rev. Mod. Phys. **66**, 1125 (1994).
[4] M. P. A. Fisher, Phys. Rev. Lett. **62**, 1415 (1989).
[5] D. R. Nelson and V. M. Vinokur, Phys. Rev. Lett. **68**, 2398 (1992); A. I. Larkin and V. M. Vinokur, *ibid.* **75**, 4666 (1995).
[6] V. Selvamanickam, M. Mironova, S. Son, and K. Salama, Physica C **208**, 238 (1993).
[7] L. Civale, A. D. Marwick, T. K. Worthington, M. A. Kirk, J. R. Thompson, L. Krusin-Elbaum, Y. Sun, J. R. Clem, and F. Holtzberg, Phys. Rev. Lett. **67**, 648 (1991); V. Hardy *et al.*, Physica C **191**, 85 (1992).
[8] J. R. Thompson, L. Krusin-Elbaum, D. K. Christen, K. J. Song, M. Paranthaman, J. L. Ullman, J. Z. Wu, Z. F. Ren, J. H. Wang, J. E. Tkaczyk, and J. A. DeLuca, Appl. Phys. Lett. **71**, 536 (1997).
[9] For a topical review, see L. Civale, Supercond. Sci. Technol. **10**, 29 (1997).
[10] L. Balents and M. Kardar, Phys. Rev. B **49**, 13 030 (1994).
[11] D. Bourgault, S. Bouffard, M. Toulemonde, D. Groult, J. Provost, F. Studer, N. Nguyen, and B. Raveau, Phys. Rev. B **39**, 6549 (1989).
[12] W. K. Kwok, U. Welp, G. W. Crabtree, K. G. Vandervoort, R. Hulscher, and J. Z. Liu, Phys. Rev. Lett. **64**, 966 (1990).
[13] J. Z. Liu, Y. X. Jia, R. N. Shelton, and M. J. Fluss, Phys. Rev. Lett. **66**, 1354 (1991); A. Zhukov, G. K. Perkins, J. V. Thomas, A. D. Caplin, H. Kupfer, and T. Wolf Phys. Rev. B **56**, 348 (1997).
[14] D. Braithwaite, D. Bourgault, A. Sulpice, J. M. Barbut, R. Tournier, I. Monot, M. Lepropre, J. Provost, and G. Desgardin, J. Low Temp. Phys. **91**, 1 (1993).
[15] I. Maggio-Aprile, C. Renner, A. Erb, E. Walker, and O. Fischer, Nature (London) **390**, 489 (1997).
[16] C. A. Duran, P. L. Gammel, R. Wolfe, V. J. Fratello, D. J. Bishop, J. P. Rice, and D. M. Ginsberg, Nature (London) **357**, 474 (1992).
[17] G. Deutscher and K. A. Müller, Phys. Rev. Lett. **59**, 1745 (1987).
[18] T. Hwa, D. R. Nelson, and V. M. Vinokur, Phys. Rev. B **48**, 1167 (1993).
[19] H. Safar, S. R. Foltyn, Q. X. Jia, and M. P. Maley, Philos. Mag. B **74**, 647 (1996).
[20] P. Gautier-Picard, E. Beaugnon, and R. Tournier Physica C **276**, 35 (1997).
[21] L. G. Schulz, J. Appl. Phys. **20**, 1030 (1954).
[22] P. Gautier Picard, Ph.D. thesis, U.J.F., 1998.
[23] D. Müller and H. C. Freyhardt, Philos. Mag. Lett. **73**, 913 (1996).
[24] M. Mironova, D. P. Lee, V. Selvamanickam, and K. Salama, Philos. Mag. A **71**, 855 (1995).
[25] M. Oussena, P. A. J. de Groot, and S. J. Porter, Phys. Rev. B **51**, 1389 (1995).
[26] D. Shi, M. S. Boley, J. G. Chen, M. Tang, U. Welp, W. K. Kwok, and B. Malecki, Supercond. Sci. Technol. **2**, 255 (1989).
[27] O. Fischer (private communication): thickness around 20 Å evaluated by STEM.
[28] M. Charalambous, J. Chaussy, and P. Lejeay, Phys. Rev. B **45**, 5091 (1992).
[29] E. M. Gyorgy, R. B. van Dover, L. F. Schneemeyer, A. E. White, H. M. O'Bryan, R. J. Felder, J. V. Waszczak, W. W. Rhodes, and F. Hellman, Appl. Phys. Lett. **56**, 2465 (1990).
[30] For a topical review of J_c determined by magnetic measurements, see, for example, S. Senoussi, J. Phys. III **2**, 1041 (1992).
[31] P. Sandiumenge, B. Martinez, and X. Obradors, Supercond. Sci. Technol. **10**, 93 (1997).
[32] B. Sonin, Phys. Rev. B **48**, 10 487 (1993).
[33] S. Sanfilippo, D. Bourgault, C. Villard, R. Tournier, P. Gautier Picard, E. Beaugnon, A. Sulpice, Th. Fournier, and P. Germi, Europhys. Lett. **39**, 657 (1997).
[34] For a review see, for example, D. E. Farrell (unpublished).

[35] S. Fleshler, W. K. Kwok, U. Welp, V. M. Vinokur, M. K. Smith, J. Downey, and G. W. Crabtree, Phys. Rev. B **47**, 14 448 (1993).
[36] W. K. Kwok *et al.*, Physica B **197**, 579 (1994).
[37] G. W. Crabtree, J. Fendrich, W. K. Kwok, and B. G. Glagola, Physica C **235–240**, 2643 (1994).
[38] T. Hwa, P. Le Doussal, D. R. Nelson, and V. M. Vinokur, Phys. Rev. Lett. **71**, 3545 (1993); P. Le Doussal and D. R. Nelson, Physica C **232**, 69 (1996).
[39] D. Lopez, L. Krusin-Elbaum, H. Safar, V. M. Vinokur, A. D. Marwich, J. Z. Sun, and C. Field, Phys. Rev. Lett. **79**, 4258 (1997); S. Hebert , V. Hardy, G. Villard, M. Hervieu, C. Simon, and J. Provost, Phys. Rev. B **57**, 649 (1998).
[40] C. Marchetti and D. R. Nelson, Phys. Rev. B **42**, 9938 (1990).
[41] F. Sandiumenge, N. Vilalta, S. Pinol, B. Martinez, and X. Obradors, Phys. Rev. B **51**, 645 (1995).
[42] H. Fujimoto, T. Taguchi, M. Murakami, and N. Koshizuka, Physica C **211**, 393 (1993).
[43] A. M. Campbell and E. J. Evetts, Adv. Phys. **21**, 199 (1972).
[44] M. V. Feigelman and V. M. Vinokur, Phys. Rev. B **41**, 8996 (1990).
[45] G. Blatter, J. Rhyner, and V. M. Vinokur, Phys. Rev. B **43**, 7826 (1991).
[46] W. Jiang, N. C. Yeh, D. S. Reed, U. Kriplani, D. A. Beam, M. Konczykowski, T. A. Tombrello, and F. Holtzberg, Phys. Rev. Lett. **72**, 550 (1994).
[47] L. Krüsin-Elbaum, L. Civale, G. Blatter, A. D. Marwick, F. Holtzberg, and C. Field, Phys. Rev. Lett. **72**, 1914 (1994).
[48] I. F. Lyuksyutov, Europhys. Lett. **20**, 273 (1992).
[49] Z. Zao, S. Yoon, H. Dai, S. Fan, and C. M. Lieber, Nature (London) **371**, 777 (1994).
[50] T. Schuster, H. Kuhn, M. Indenbom, M. Leghissa, M. Kraus, and M. Konczykowski, Phys. Rev. B **51**, 16 358 (1995).
[51] L. Civale, L. Krüsin-Elbaum, J. R. Thompson, R. Wheeler, A. D. Marwick, M. A. Kirk, Y. R. Sun, F. Holtzberg, and C. Field, Phys. Rev. B **50**, 4102 (1994).
[52] W. K. Kwok, J. A. Fendrich, V. M. Vinokur, A. E. Koshelev, G. W. Crabtree, Phys. Rev. Lett. **76**, 4596 (1996).
[53] D. R. Nelson and V. M. Vinokur, Phys. Rev. B **48**, 13 060 (1993).